Restricted Isometry and Information-Based Numerical Analysis

for the Degree of Doctor of Philosophy

Hao-Ning Wu
The University of Hong Kong
June 26, 2023

Overview

- Motivation and terms explained - Chapter 1
  - numerical analysis, information-based, and restricted isometry
- Polynomial approximation - Chapters 2–4
  - hyperinterpolation, quadrature, and singular/oscillatory functions
- Numerical solutions to PDEs - Chapter 5
  - spectral methods, Allen–Cahn equation, and maximum principles
- Compressed sensing and imaging - Chapters 6–7
  - compressed sensing, image reconstruction, and new regularization

Lloyd N. Trefethen (SIAM News, Nov 1992)

Numerical analysis is the study of algorithms for the problems of continuous mathematics.

e.g., approximating f, solving $Lu = f$ for u, minimizing f, ...

discretization $\downarrow$ samples $\{f(x_j)\}$

Information-based numerical analysis is the study of algorithms for the problems of continuous mathematics without full access to the concerned objects but only partial, contaminated, and priced information.

You can add qualifications, $\cdots$, but this definition is the essence of the matter, and the spotlight is on algorithms, not rounding errors. If rounding errors vanished, 90% of numerical analysis would remain.

- Trefethen: An Applied Mathematician's Apology (2022)

Information-based situations

The term **information-based** refers to situations where the information (e.g. samples) is

- **partial** - we cannot solve the continuous mathematics problem exactly and uniquely with the information at hand
- **contaminated** - the information is processed with errors (e.g. sampling noise and rounding errors)
- **priced** - we are charged for each sample

- Claude Shannon and information theory? Not the same.
- Information-based complexity (IBC)? Partly the same.
  - IBC optimizes total cost (incl. sampling and computation)
  - We explore reasonable error bounds under information-based situations

Toy example: M. J. D. Powell (1936 – 2015) and derivative-free opt'

Given an **oracle** (no first-order information, let alone the second) $f : \mathbb{R}^d \to \mathbb{R}$, how to solve

$$\min_{x \in \mathbb{R}^d} \; f(x)$$

with function evaluations only, referred to as the **derivative-free optimization**?

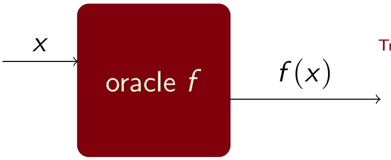

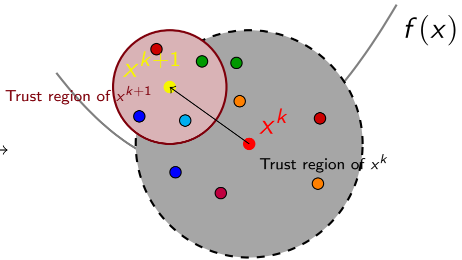

Fun fact: both illustrations were designed by ChatGPT.

Yet another term: restricted isometry

We assume **restricted isometry** of our samples.

- For numerical integration $\sum_{j=1}^{m} w_j f(x_j) \approx \int_\Omega f(x) d\omega(x)$:

Marcinkiewicz–Zygmund property (1937)

For all $\chi \in \mathbb{P}_n$, there exists an $\eta \in [0,1)$ such that
$(1-\eta)\int_\Omega \chi^2 \mathrm{d}\omega_d \leq \sum_{j=1}^{m} w_j \chi(x_j)^2 \leq (1+\eta)\int_\Omega \chi^2 \mathrm{d}\omega_d$.

- For sub-sampling $A \in \mathbb{R}^{m\times n} : \mathbb{R}^n \to \mathbb{R}^m$ $(m \leq n)$:

Restricted isometry property (Candès & Tao 2005)

For all s-sparse $x \in \mathbb{R}^n$, there exists a $\delta_s \in (0,1)$ such that $(1-\delta_s)\|x\|_2^2 \leq \|Ax\|_2^2 \leq (1+\delta_s)\|x\|_2^2$.

- **Polynomial interpolation**: complicated in multivariate cases

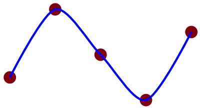

- **Least squares (LS) approximation**: hard to analyze unless obtaining the minimizer's explicit form

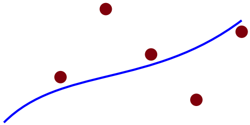

- **Orthogonal projection**: non-implementable on computers

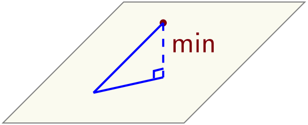

Ian H. Sloan (in the early 1990s): Does the interpolation of functions on $\mathbb{S}^1$ have properties as good as orthogonal projection?

✍ Sloan ('95 JAT)

- on $\mathbb{S}^1$: Yes.
- on $\mathbb{S}^d$ ($d \geq 2$) and most high-dim regions: remaining **Problematic** to this day!
- Using more points than interpolation? $\rightarrow$ **hyper**interpolation

Photo taken from the Red Centre, UNSW Sydney.

- $\Omega \subset \mathbb{R}^d$: general compact region
- $\mathbb{P}_n$: space of polynomials of degree $\leq n$ over Ω; $d_n := \dim \mathbb{P}_n$
- $\{p_1, p_2, \ldots, p_{d_n}\}$: orthonormal basis of $\mathbb{P}_n$

The **orthogonal projection** of $f \in C(\Omega)$ onto $\mathbb{P}_n$ is defined as $\mathcal{P}_n f := \sum_{\ell=1}^{d_n} \langle f, p_\ell \rangle p_\ell$, where $\langle f, g \rangle = \int_\Omega fg \mathrm{d}\omega$.

The **hyperinterpolation** of $f \in C(\Omega)$ onto $\mathbb{P}_n$ is defined as

$$\mathcal{L}_n f := \sum_{\ell=1}^{d_n} \langle f, p_\ell \rangle_m p_\ell,$$

where $\langle f, g \rangle_m := \sum_{j=1}^{m} w_j f(x_j) g(x_j)$ with all $w_j > 0$.

- $\mathcal{L}_n f$ is a discretized version of $\mathcal{P}_n f$.
- $\mathcal{L}_n f$ is the minimizer of a discrete LS problem:

$$\mathcal{L}_n f = \arg\min_{p \in \mathbb{P}_n} \sum_{j=1}^{m} w_j [f(x_j) - p(x_j)]^2.$$

- $\mathcal{L}_n f$ reduces to interpolation ($\mathcal{L}_n f(x_j) = f(x_j)$, $j = 1, \dots, m$) if the quadrature rule is **minimal**: an m-pt quadrature is *minimal* if $m = d_n$ and its **exactness degree** exceeds $2n$.

The quadrature rule $\sum_{j=1}^{m} w_j g(x_j) \approx \int_\Omega g \mathrm{d}\omega$ is said to have **exactness degree** $2n$ if

$$\sum_{j=1}^{m} w_j g(x_j) = \int_\Omega g \mathrm{d}\omega \quad \forall g \in \mathbb{P}_{2n}.$$

Caveat: minimal quadrature rules can be ONLY constructed on a few low-dimensional Ω, such as $[-1,1]$, $[-1,1]^2$, and $\mathbb{S}^1$.
No minimal quadrature rules are constructed on $[-1,1]^d$ ($d \geq 3$) or $\mathbb{S}^d$ ($d \geq 2$).

The theory of hyperinterpolation was established under the assumption of quadrature exactness degree.

Theorem (Sloan 1995)

Assume the involved quadrature rule has exactness degree $2n$. Then for any $f \in C(\Omega)$, its hyperinterpolant $\mathcal{L}_n f$ satisfies:

- $\mathcal{L}_n \chi = \chi$ for any $\chi \in \mathbb{P}_n$;
- $\langle \mathcal{L}_n f - f, \chi \rangle_m = 0$ for all $\chi \in \mathbb{P}_n$;
  (cf. $\langle \mathcal{P}_n f - f, \chi \rangle = 0 \ \forall \ \chi \in \mathbb{P}_n$)
- $\|\mathcal{L}_n f\|_2 \leq V^{1/2} \|f\|_\infty$;
- $\|\mathcal{L}_n f - f\|_2 \leq 2V^{1/2} E_n(f)$.

Here $V = |\Omega|$ and $E_n(f) := \inf_{\chi \in \mathbb{P}_n} \|f - \chi\|_\infty$.

Remark: No $L^2 \to L^2$ theory but only $C \to L^2$ (explained later).

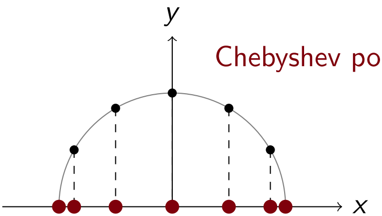

Clenshaw–Curtis quad (1960)
$n+1$ points $\to$ n exactness degree

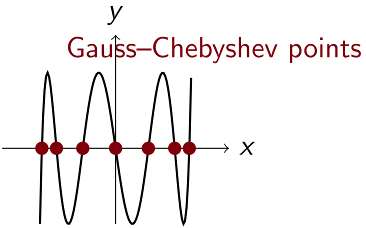

Gauss–Chebyshev quad (19th century)
$n+1$ points $\to$ $2n+1$ exactness degree

✍ Trefethen ('08 SIREV): entered the complex plane and demonstrated for most functions, the Clenshaw–Curtis and Gauss quadrature rules have comparable accuracy

✍ Trefethen ('22 SIREV): numerical integral is an analysis topic, while quadrature exactness is an algebraic matter

Recall the **Marcinkiewicz–Zygmund (MZ) property**

$$(1-\eta)\int_{\Omega}\chi^2\mathrm{d}\omega_d \leq \sum_{j=1}^{m} w_j\chi(x_j)^2 \leq (1+\eta)\int_{\Omega}\chi^2\mathrm{d}\omega_d \quad \forall\chi\in\mathbb{P}_n.$$

What if **relaxing** $2n$ to, say, $n+k$ with $0<k\leq n$?

Theorem 2.2.8

Assume the quadrature rule has exactness degree $n+k$ and **satisfies the MZ property**. Then for any $f\in C(\Omega)$:

- $\mathcal{L}_n\chi=\chi$ for any $\chi\in\mathbb{P}_k$;
- $\langle\mathcal{L}_n f-f,\chi\rangle_m=0$ for all $\chi\in\mathbb{P}_k$;
- $\|\mathcal{L}_n f\|_2\leq\dfrac{V^{1/2}}{\sqrt{1-\eta}}\|f\|_\infty$;
- $\|\mathcal{L}_n f-f\|_2\leq\left(\dfrac{1}{\sqrt{1-\eta}}+1\right)V^{1/2}E_k(f)$.

Why Marcinkiewicz–Zygmund?

- The key observation to show the stability of $\mathcal{L}_n f$ (with exact.):

$$\|\mathcal{L}_n f\|_2^2 + \underbrace{\langle f - \mathcal{L}_n f, f - \mathcal{L}_n f\rangle_m}_{\geq 0 \ (\text{why all } w_j > 0)} = \langle f, f\rangle_m = \underbrace{\sum_{j=1}^m w_j f(x_j)^2 \leq V\|f\|_\infty^2}_{\text{why } C \to L^2 \text{ theory only}}$$

- When the quad exactness degree is $n+k$ $(0 < k \leq n)$:

$$\|\mathcal{L}_n f\|_2^2 + \underbrace{\langle f - \mathcal{L}_n f, f - \mathcal{L}_n f\rangle_m + \sigma_{m,n,f}}_{\geq 0?} = \langle f, f\rangle_m;$$

$$\sigma_{n,k,f} = \langle \mathcal{L}_n f - \mathcal{L}_k f, \mathcal{L}_n f - \mathcal{L}_k f\rangle - \langle \mathcal{L}_n f - \mathcal{L}_k f, \mathcal{L}_n f - \mathcal{L}_k f\rangle_m.$$

- Note that $\mathcal{L}_n f - \mathcal{L}_k f \in \mathbb{P}_n$, the **MZ property** implies

$$|\sigma_{n,k,f}| \leq \eta \langle \mathcal{L}_n f - \mathcal{L}_k f, \mathcal{L}_n f - \mathcal{L}_k f\rangle.$$

Numerical results on $[-1, 1]$

p_ℓ: normalized Legendre polynomials; $d_n = \dim \mathbb{P}_n = n + 1$

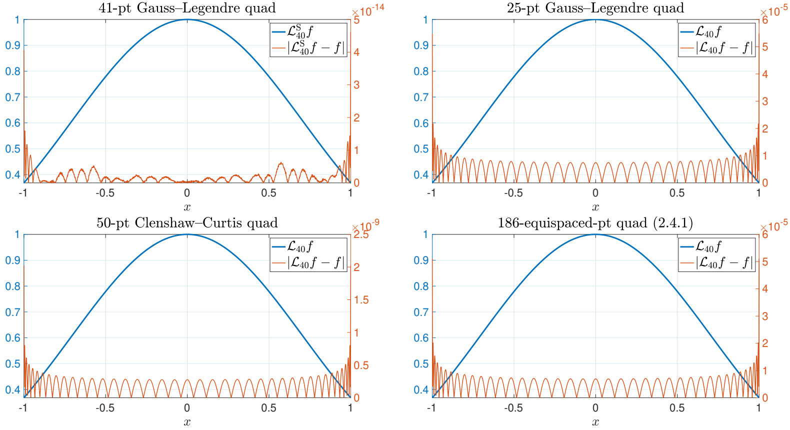

Figure: Hyperinterpolants $\mathcal{L}_{40}^{\mathrm{S}} f$ and $\mathcal{L}_{40} f$ of $f = \exp(-x^2)$, constructed by various quadrature rules.

Numerical results on $\mathbb{S}^2$

Delsarte, Goethals, and Seidel 1977

A point set $\{x_1, x_2, \dots, x_m\} \subset \mathbb{S}^2$ is said to be a **spherical t-design** if it satisfies

$$\frac{1}{m}\sum_{j=1}^{m} g(x_j) = \frac{1}{4\pi}\int_{\mathbb{S}^2} g \,\mathrm{d}\omega \quad \forall g \in \mathbb{P}_t.$$

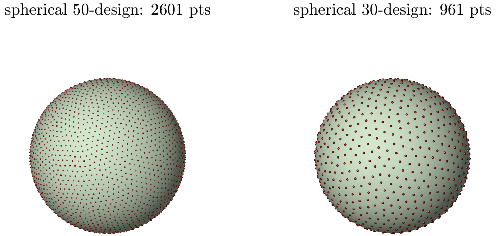

Figure: Spherical 50- and 30-designs, generated by the method proposed by An, Chen, Sloan, and Womersley (2010).

p_ℓ: spherical harmonics; $d_n = \dim \mathbb{P}_n = (n+1)^2$

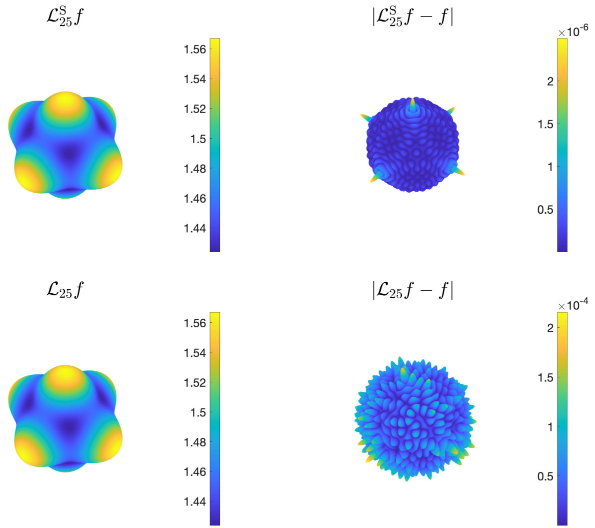

Figure: Hyperinterpolants $\mathcal{L}_{25}^{\mathrm{S}} f$ and $\mathcal{L}_{25} f$ of a Wendland function, constructed by spherical t-designs with $t = 50$ (upper row) and 30 (lower row).

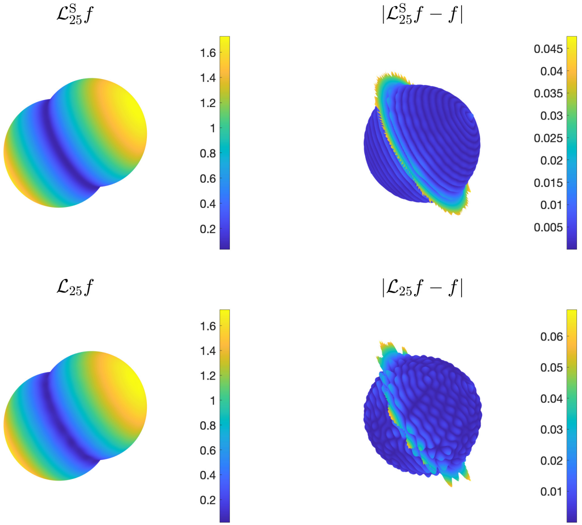

Figure: Hyperinterpolants $\mathcal{L}_{25}^{\mathrm{S}} f$ and $\mathcal{L}_{25} f$ of $f(\mathbf{x}) = f(x, y, z) = |x + y + z|$, constructed by spherical t-designs with $t = 50$ (upper row) and 30 (lower row).

Contributions in Chapter 3: Hyperinterpolation of singular/oscillatory functions

Why a **higher** hyperinterpolation **degree** is desired even if the quadrature exactness is not enough: an application

How to approximate functions of the form $F(x) = K(x)f(x)$?
- ➥ $K \in L^1(\Omega)$, which needs not be continuous or of one sign
- ➥ $f \in C(\Omega)$ (and preferably smooth)

Example: fundamental solutions of the Helmholtz equation

$$G(x,y) = \begin{cases} \dfrac{i}{4} H_0^{(1)}(\kappa|x-y|) & \text{for } x, y \in \mathbb{R}^2 \\ \dfrac{1}{4\pi}\dfrac{e^{i\kappa|x-y|}}{|x-y|} & \text{for } x, y \in \mathbb{R}^3 \end{cases}$$

❑ $\mathcal{P}_n F := \sum_{\ell=1}^{d_n} \langle Kf, p_\ell \rangle p_\ell$ or $\mathcal{L}_n F := \sum_{\ell=1}^{d_n} \langle Kf, p_\ell \rangle_m p_\ell$
To evaluate, by classical quadrature rules, the integrals

$$\langle Kf, p_\ell \rangle = \int_\Omega K(x) f(x) p_\ell \mathrm{d}\omega(x)$$

is **inefficient**.

Instead, a **semi-analytical way** for $\int_\Omega K(x)f(x)\mathrm{d}\omega(x)$:

1. Replace f by its interpolant or approximant $\sum_{\ell=1}^{d_n} c_\ell p_\ell$;
2. Evaluate the integral by

$$\int_\Omega K(x)f(x)\mathrm{d}\omega(x) \approx \sum_{\ell=1}^{d_n} c_\ell \int_\Omega K(x)p_\ell(x)\mathrm{d}\omega(x);$$

3. Assume the **modified moments** $\int_\Omega K(x)p_\ell(x)\mathrm{d}\omega(x)$ can be evaluated analytically or stably by some iterative subroutines.
   ▻ Let us make this assumption from now on.

Efficient hyperinterpolation

$$\mathcal{S}_n F := \sum_{\ell=1}^{d_n} \left(\int_\Omega K(\mathcal{L}_n f) p_\ell \mathrm{d}\omega \right) p_\ell.$$

4. We need to evaluate $\int_\Omega K(x)p_\ell(x)p_{\ell'}(x)\mathrm{d}\omega(x)$ for $\mathcal{S}_n F$, then additionally represent $p_\ell(x)p_{\ell'}(x)$ by an orthonormal basis.

Theorem 3.5.4

Assume the quadrature rule has exactness degree $n+k$ and **satisfies the MZ property**. Then for any $f \in C(\Omega)$:

- Let $K \in C(\Omega)$. $\|\mathcal{S}_n F\|_2 \leq \frac{V^{1/2}}{\sqrt{1-\eta}} \|K\|_\infty \|f\|_\infty$;
- Let $K \in C(\Omega)$. $\|\mathcal{S}_n F - F\|_2 \leq$
$$\left(\frac{V^{1/2}}{\sqrt{1-\eta}}\|K\|_\infty + \|K\|_2\right) E_k(f) + 2V^{1/2} E_n(K\chi^*).$$

Here $\chi^* \in \mathbb{P}_k$ is the best uniform approximation of f in $\mathbb{P}_k$.

(We also have analysis for $K \in L^1$ and L^2)

Considering $\mathcal{L}_n F = \mathcal{L}_n(Kf)$, we have $\|\mathcal{L}_n F - F\|_2 \lesssim E_k(Kf)$.

Comparison:

$\mathcal{S}_n F$	$\mathcal{L}_n F$
$E_k(f)$ & $E_n(K\chi^*)$	$E_k(Kf)$

Numerical results on [-1,1]

- $K(x) = e^{i\kappa x}$ with $\kappa > 0$.
- Filon–Clenshaw–Curtis rule (Domínguez, Graham, and Smyshlyaev 2011) for modified moments β_r.

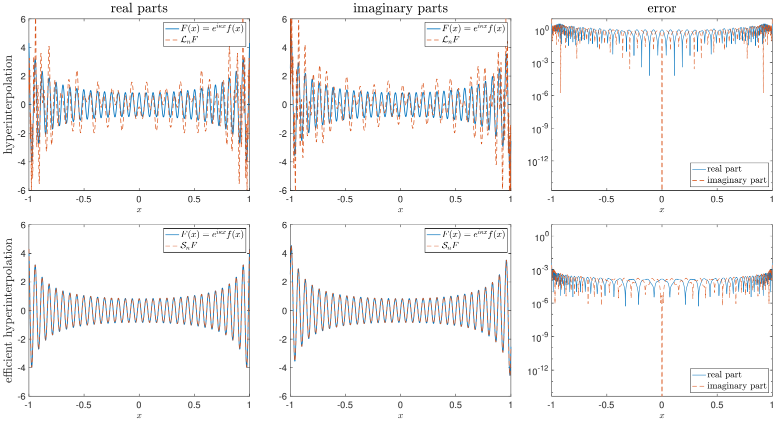

Figure: Approximation of $F(x) = e^{i\kappa x}(1.2 - x^2)^{-1}$ by $\mathcal{L}_n$ and $\mathcal{S}_n$ with $(\kappa, n, m) = (100, 120, 70)$.

➥ Spherical harmonics $Y_{\ell,k}$ themselves are oscillatory!

➥ Using high-order spherical t-designs to evaluate the modified moments analytically.

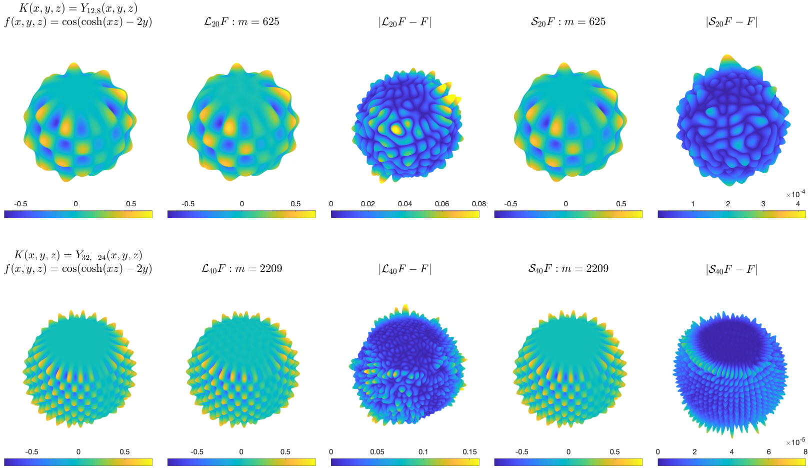

Figure: Approximation of $F(x) = Y_{\ell,k}(x,y,z)\cos(\cosh(xz) - 2y)$ by $\mathcal{L}_n$ and $\mathcal{S}_n$.

A case study on **spheres**: The polynomial space $\mathbb{P}_n(\mathbb{S}^d)$ is the span of spherical harmonics

$$\{Y_{\ell,k} : \ \ell = 0, 1, \ldots, n, \ \ k = 1, 2, \ldots, Z(d, \ell)\};$$

$\mathbb{P}_n(\mathbb{S}^d)$ is also a **reproducing kernel Hilbert space** with the reproducing kernel

$$G_n(x, y) = \sum_{\ell=0}^{n} \sum_{k=1}^{Z(d,\ell)} Y_{\ell,k}(x) Y_{\ell,k}(y)$$

in the sense that $\langle \chi, G(\cdot, x)\rangle = \chi(x)$ for all $\chi \in \mathbb{P}_n(\mathbb{S}^d)$.

For hyperinterpolation $\mathcal{L}_n$:

$$\begin{aligned}\mathcal{L}_n f(x) &= \sum_{\ell=0}^{n} \sum_{k=1}^{Z(d,\ell)} \left(\sum_{j=1}^{m} w_j f(x_j) Y_{\ell,k}(x_j) \right) Y_{\ell,k}(x) \\ &= \sum_{j=1}^{m} w_j f(x_j) G_n(x, x_j)\end{aligned}$$

Theorem 4.3.2

Assume the quadrature rule **satisfies the MZ property**. Then for any $f \in C(\mathbb{S}^d)$:

- $\|\mathcal{U}_n f\|_{L^2} \leq \sqrt{1+\eta}\left(\sum_{j=1}^m w_j\right)^{1/2} \|f\|_\infty$;
- $\|\mathcal{U}_n f - f\|_{L^2} \leq \left(\sqrt{1+\eta}\left(\sum_{j=1}^m w_j\right)^{1/2} + |\mathbb{S}^d|^{1/2}\right) E_n(f)$ $+ \sqrt{\eta^2+4\eta}\|\chi^*\|_{L^2}$.

Notation: $\mathcal{U}_n$ for hyperinterpolation without quadrature exactness

Note: If the quadrature rule has exactness degree at least **1**, then

$$\sum_{j=1}^m w_j = \int_{\mathbb{S}^d} 1 \mathrm{d}\omega_d = |\mathbb{S}^d|.$$

Controlling the constant η

Mhaskar, Narcowich, and Ward 2001

The **MZ property** holds for $\mathcal{X}_m := \{x_1, \ldots, x_m\} \subset \mathbb{S}^d$ if $N \lesssim \frac{\eta}{2h_{\mathcal{X}_m}}$, where $h_{\mathcal{X}_m} := \max_{x \in \mathbb{S}^{d-1}} \min_{x_j \in \mathcal{X}_m} \mathrm{dist}(x, x_j)$ is the **mesh norm** of $\mathcal{X}_m$ and $\mathrm{dist}(x, y)$ denotes the geodesic distance.

Le Gia and Mhaskar 2009

If the quadrature rule is equal-weight and the quadrature points are i.i.d drawn from the distribution ω_d, then there exists a constant $\bar{c} := \bar{c}(\gamma)$ such that the **MZ property** holds with probability exceeding $1 - \bar{c}N^{-\gamma}$ on the condition

$$m \geq \bar{c}\frac{N^d \log N}{\eta^2}.$$

Error bound investigated numerically

- The error bound is controlled by n and m.
- Le Gia & Mhaskar (random points)
  - $\rightarrow$ η has a lower bound order $\sqrt{n^2 \log n / m}$
  - $\rightarrow$ $\sqrt{\eta^2 + 4\eta}\|\chi^*\|_{L^2}$ has a lower bound of order $m^{-1/4}$

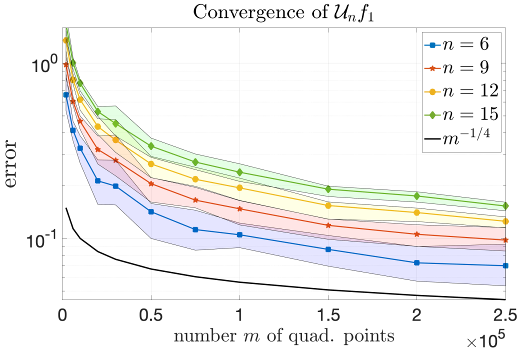

Figure: Approximating $f_1(x) = (x_1 + x_2 + x_3)^2 \in \mathbb{P}_6(\mathbb{S}^2)$.

- $f_2(x_1,x_2,x_3) := |x_1+x_2+x_3| + \sin^2(1+|x_1+x_2+x_3|)$
- The Franke function for the sphere

$$\begin{aligned} f_3(x_1,x_2,x_3) :=\, & 0.75\exp(-((9x_1-2)^2)/4-((9x_2-2)^2)/4-((9x_3-2)^2)/4) \\ & +0.75\exp(-((9x_1+1)^2)/49-((9x_2+1))/10-((9x_3+1))/10) \\ & +0.5\exp(-((9x_1-7)^2)/4-((9x_2-3)^2)/4-((9x_3-5)^2)/4) \\ & -0.2\exp(-((9x_1-4)^2)-((9x_2-7)^2)-((9x_3-5)^2)) \in C^\infty(\mathbb{S}^2) \end{aligned}$$

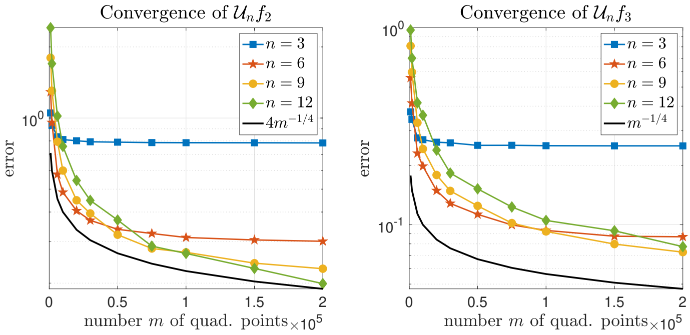

Figure: Approximating f_2 and f_3.

To compute smooth solutions of **semi-linear PDEs** on $\mathbb{S}^{d-1} \subset \mathbb{R}^d$ with dimension $d \geq 3$ of the form

$$u_t = \boldsymbol{L}u + \boldsymbol{N}(u), \quad u(0,x) = u_0(x),$$

where $\boldsymbol{L}$ is a constant-coefficient linear differential operator, and $\boldsymbol{N}$ is a constant-coefficient nonlinear differential (or non-differential) operator of lower order.

Example: **Allen–Cahn equation**

$$u_t = \nu^2 \Delta u - F'(u), \quad u(0,x) = u_0(x),$$

where $F'(u) = f(u) = u^3 - u$.

- energy stability: $\mathcal{E}(u(t,\cdot)) \leq \mathcal{E}(u(s,\cdot))$ for $s \leq t < \infty$ with
$$\mathcal{E}(u) := \int_{\mathbb{S}^{d-1}} \left(\frac{1}{2}\nu^2 |\nabla u|^2 + F(u) \right) \mathrm{d}\omega_d$$
- maximum principle: the entire solution is bounded by $\|u_0\|_\infty$

Motivations:

1. Remove stringent and technical conditions (e.g. $\tau \ll 1$ and $\sup_u |F''(u)| \leq L$) in numerical schemes
   $\rightarrow$ effective maximum principle (D. Li 2021) $\rightarrow$ energy stability
2. Investigate the behavior of numerical solutions under quadrature rules
3. Information-based situations

Our idea in a nutshell: **linearizing** the nonlinear part $\boldsymbol{N}(u)$ by hyperinterpolation:

$$\begin{cases} \dfrac{u^{n+1} - u^n}{\tau} = \nu^2 \Delta u^{n+1} - \mathcal{L}_N \left((u^n)^3 - u^n \right), \quad n \geq 0, \\ u^0 = \mathcal{L}_N u_0 \end{cases}$$

where $\tau > 0$ is the time step.

For each time iteration: using $-\Delta Y_{\ell,k} = \ell(\ell + d - 2) Y_{\ell,k}$, only need to solve a **linear system**.

Theorems 5.3.1 & 5.3.3: L^∞ stability and effective maximum principle for $\tau \leq 1/2$

Let $0 < \alpha_0 \leq 1$ and $s_0 \geq \frac{d-1}{2}$. **Assume** $u_0 \in H^s(\mathbb{S}^{d-1})$ with $s > d-1$ and $\|u_0\|_\infty \leq 1$. **Control** $\eta = \tilde{c}N^{-\varepsilon}$ for any $\tilde{c} \geq 0$ and $\varepsilon > s_0$. If $N \geq N_1 := N_1(\alpha_0, \nu, s, d, u_0, \varepsilon)$, then

$$\sup_{n\geq 0} \|u^n\|_\infty \leq 1 + \alpha_0.$$

If $N \geq N_2 := N_2(\nu, s, d, u_0, \varepsilon)$, then for any $n \geq 1$,

$$\|u^n\|_\infty \leq 1 + \theta^n \alpha_0 + \frac{1-\theta^n}{1-\theta}\tau C_{\nu,u_0,s,d}\left(\sqrt{1+\eta}N^{d-1-s}\right. \cdot \\ \left. + \eta N^{s_0+\frac{d-1}{2}-s} + \eta N^{s_0}\right),$$

where $\theta = 1 - 2\tau$.

Idea of proof:

- Induction for n;
- For each induction:

➥ Using the best approximation error estimate (Ragozin 1971) with the Sobolev embedding into Hölder spaces (note that $E_N(f)$ is defined by $\|\cdot\|_\infty$, while Sobolev spaces here $\|\cdot\|_{L^2}$):

$$E_N(f) \leq \frac{c_3(f)}{N^{s-\frac{d-1}{2}}}\|f\|_{H^s};$$

➥ Using discrete smoothing technique (bootstrapping) for the boundedness of $\|u^n\|_{H^s}$.

Theorem 5.3.6: L^∞ stability for $1/2 < \tau < 2$

Let $1/2 < \tau \leq 2 - \epsilon_0$ for some $0 < \epsilon_0 \leq 1$,

$$M_0 = \frac{1}{2}\left(\frac{(1+\tau)^{3/2}}{\sqrt{3\tau}} \cdot \frac{2}{3} + \sqrt{\frac{2+\tau}{\tau}}\right),$$

and $s_0 \geq (d-1)/2$. **Assume** $u_0 \in H^s(\mathbb{S}^{d-1})$ with $s > d-1$ and $\|u^0\|_\infty \leq M_0$. **Control** $\eta = \tilde{c}N^{-\varepsilon}$ for any $\tilde{c} \geq 0$ and $\varepsilon > s_0$. If $N \geq N_3 := N_3(\epsilon_0, \nu, s, d, u_0, \varepsilon)$, then

$$\sup_{n\geq 0} \|u^n\|_\infty \leq M_0.$$

No effective maximum principle derived.

Idea of proof:

- Induction for n again;
- For each induction, using lemma by Li to bound $\|p(u^n)\|_\infty$, where $p(x) = (1+\tau)x - \tau x^3$.

- If the quadrature rule has exactness degree $2N$, our scheme for $u_t = \boldsymbol{L}u + \boldsymbol{N}(u)$ is equivalent to a **discrete Galerkin scheme**

$$\frac{1}{\tau}\left\langle u^{n+1} - u^n, \chi \right\rangle_m = \left\langle \boldsymbol{L}u^{n+1}, \chi \right\rangle_m + \langle \boldsymbol{N}(u^n), \chi \rangle_m \quad \forall \chi \in \mathbb{P}_N.$$

Corollary 5.4.1: Additionally assuming the quad. exact. $2N$

- ***L^∞* stability for $\tau \leq 1/2$.** If $N \geq N_4(\alpha_0, \nu, s, d, u_0)$, then $\sup_{n\geq 0} \|u^n\|_\infty \leq 1 + \alpha_0$.
- **Effective maximum principle for $\tau \leq 1/2$.** If $N \geq N_4'(\nu, s, d, u_0)$, then for any $n \geq 1$,

$$\|u^n\|_\infty \leq 1 + \theta^n \alpha_0 + \frac{1 - \theta^n}{1 - \theta} \tau C_{\nu, u_0, s, d} N^{d-1-s}.$$

- ***L^∞*-stability for $1/2 < \tau < 2$.** Let $1/2 < \tau < 2 - \epsilon_0$ for some $0 < \epsilon_0 \leq 1$. If $N \geq N_4''(\epsilon_0, \nu, s, d, u_0)$, then

$$\sup_{n\geq 0} \|u^n\|_\infty \leq M_0.$$

Lemma 5.4.3: Energy estimates

For any $n \geq 0$, if the quad exactness degree $\geq 2N$, then

$$\tilde{\mathcal{E}}(u^{n+1}) - \tilde{\mathcal{E}}(u^n) + \left(\frac{1}{\tau} + \frac{1}{2}\right) \sum_{j=1}^{m} w_j (u^{n+1}(x_j) - u^n(x_j))^2$$

$$\leq \frac{3}{2} \max\left\{\|u^n\|_\infty^2, \|u^{n+1}\|_\infty^2\right\} \sum_{j=1}^{m} w_j (u^{n+1}(x_j) - u^n(x_j))^2;$$

if the quad exactness degree $\geq 4N$, then

$$\mathcal{E}(u^{n+1}) - \mathcal{E}(u^n) + \left(\frac{1}{\tau} + \frac{1}{2}\right) \int_{\mathbb{S}^{d-1}} (u^{n+1} - u^n)^2 \mathrm{d}\omega_d$$

$$\leq \frac{3}{2} \max\left\{\|u^n\|_\infty^2, \|u^{n+1}\|_\infty^2\right\} \int_{\mathbb{S}^{d-1}} (u^{n+1} - u^n)^2 \mathrm{d}\omega_d.$$

Here $\mathcal{E}(u)$ denote the energy (previously defined) of u, and $\tilde{\mathcal{E}}(u)$ discretizes $\mathcal{E}(u)$ by the concerned quadrature rule.

- For **(discrete) energy stability**, it suffice to control $\|u^n\|_\infty$ (by L^∞ stability derived previously) such that

$$\frac{1}{\tau} + \frac{1}{2} \geq \frac{3}{2} \sup_{n\geq 0} \|u^n\|_\infty^2.$$

- **Why quadrature exactness?**
  To derive the above (discrete) energy estimates, we need

$$\left\langle f(u^n) - \mathcal{L}_N(f(u^n)), u^{n+1} - u^n \right\rangle_m = 0$$

and

$$\left\langle f(u^n) - \mathcal{L}_N(f(u^n)), u^{n+1} - u^n \right\rangle = 0,$$

respectively, which are ensured by

1) the projection property $\langle f - \mathcal{L}_N, \chi \rangle_m = 0 \ \forall \chi \in \mathbb{P}_N$ of hyperinterpolation if the quad exactness deg $\geq 2N$; and

2) $\langle f - \mathcal{L}_N, \chi \rangle = \langle f - \mathcal{L}_N, \chi \rangle_m$ if $f \in \mathbb{P}_{3N}$ and the quad exactness deg $\geq 4N$.

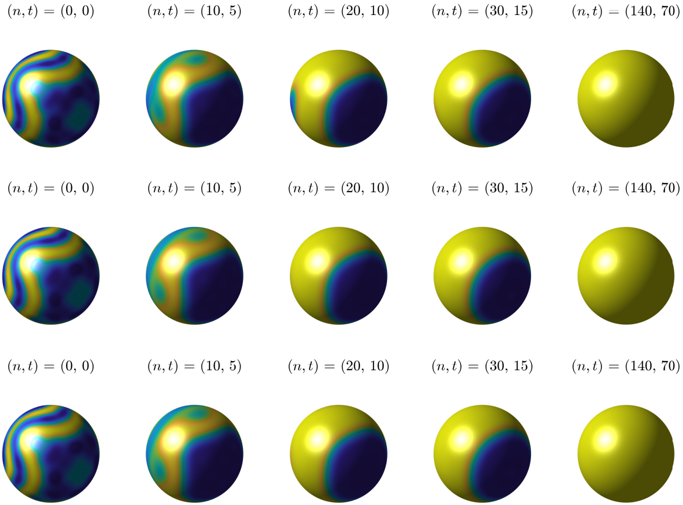

Figure: Numerical solution to the Allen–Cahn equation with $\nu = 0.1$ and initial condition $u(0, x, y, z) = \cos(\cosh(5xz) - 10y)$ using our scheme with $\tau = 0.5$, $N = 15$, and different quadrature points. From top row to bottom row: $m = \lfloor 120N^2 \ln N \rfloor = 73,117$ **random points**; $m = (2N+1)^2 = 961$ **equal area points**; and $m = 961$ **spherical $2N$-designs**.

Compressed sensing (CS) and imaging

To recovery an unknown $\bar{x} \in \mathbb{R}^n$ from $b = A\bar{x} + e \in \mathbb{R}^m$, where $A \in \mathbb{R}^{m \times n}$ with $m \ll n$, and $e \in \mathbb{R}^m$ with $\|e\|_2 \leq \tau$:

- One may consider solving the ℓ^0 minimization problem:

$$\min_{x \in \mathbb{R}^n} \|x\|_0 \quad \text{s.t.} \quad \|Ax - b\|_2 \leq \tau.$$

  Alternatively, the basis pursuit (BP) model:

$$\min_{x \in \mathbb{R}^n} \|x\|_1 \quad \text{s.t.} \quad \|Ax - b\|_2 \leq \tau.$$

- Our springback model: For $\alpha > 0$,

$$\min_{x \in \mathbb{R}^n} \|x\|_1 - \frac{\alpha}{2}\|x\|_2^2 \quad \text{s.t.} \quad \|Ax - b\|_2 \leq \tau.$$

- Standard CS theory holds for the BP model, assuming that $\bar{x}$ or its coefficients after an orthonormal transform are **sparse**:

$$\|x^{\text{opt}} - \bar{x}\|_2 \leq ?$$

  One type of theory is established under the RIP framework (**restricted isometry**).

Extending to image reconstruction: $y = \mathcal{M}\bar{X} + e \in \mathbb{C}^m$, where the unknown $\bar{X} \in \mathbb{C}^{N \times N}$, $\mathcal{M} : \mathbb{C}^{N \times N} \to \mathbb{C}^m$ with $m \ll N^2$, and $e \in \mathbb{R}^m$ with $\|e\|_2 \leq \tau$.

- BP model $\to$ total variation (TV) model ($\|X\|_{\mathrm{TV}} = \|\nabla X\|_1$):

$$\min_{X \in \mathbb{C}^{N \times N}} \|X\|_{\mathrm{TV}} \quad \text{s.t.} \quad \|\mathcal{M}X - y\|_2 \leq \tau,$$

- Springback model $\to$ enhanced TV model:

$$\min_{X \in \mathbb{C}^{N \times N}} \|X\|_{\mathrm{TV}} - \frac{\alpha}{2}\|\nabla X\|_2^2 \quad \text{s.t.} \quad \|\mathcal{M}X - y\|_2 \leq \tau,$$

- Images becomes sparse after the gradient transform ∇ (due to the low density of edges within an image), but ∇ **fails to be orthonormal** $\to$ obliged to establish image reconstruction theory from scratch.

Enhanced TV from a PDE perspective

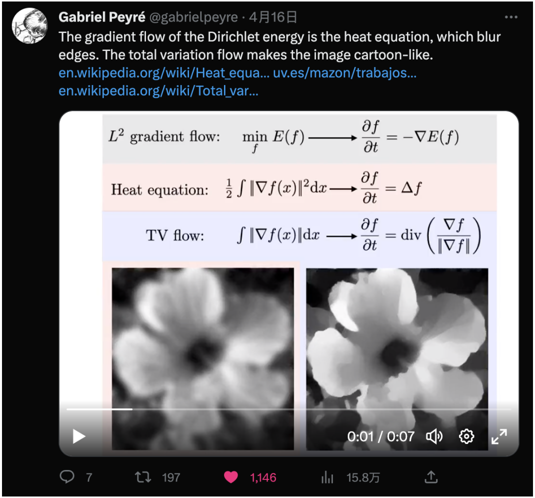

Enhanced TV flow:

$$\int \left(\|\nabla f(x)\| - \frac{\alpha}{2} \|\nabla f(x)\|^2 \right) \mathrm{d}x \to \frac{\partial f}{\partial t} = \mathrm{div}\left(\frac{\nabla f}{\|\nabla f\|} \right) - \alpha \Delta f$$

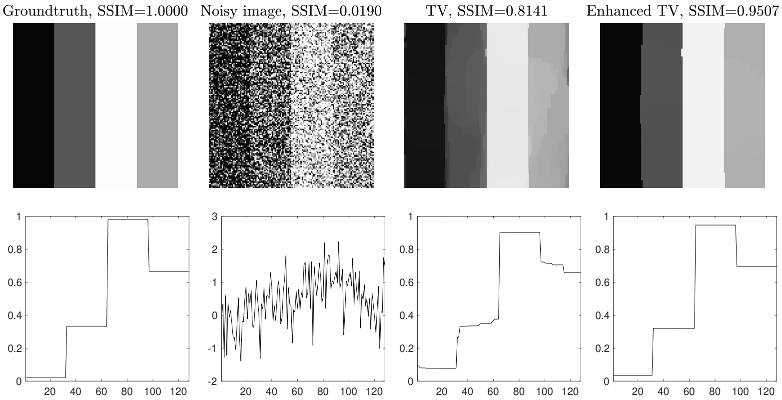

Figure: Illustration of the TV and enhanced TV regularization for image denoising. Top row: SSIM values of each image; Bottom row: intensity profiles of each image along the horizontal straight line splitting the image equally.

Restricted isometry property (RIP) recalled

For sub-sampling $A \in \mathbb{R}^{m\times n} : \mathbb{R}^n \to \mathbb{R}^m$ ($m \leq n$):

Restricted isometry property (Candès & Tao 2005)

For all s-sparse $x \in \mathbb{R}^n$, there exists a $\delta_s \in (0,1)$ such that $(1-\delta_s)\|x\|_2^2 \leq \|Ax\|_2^2 \leq (1+\delta_s)\|x\|_2^2$, and the smallest δ_s is said to be the *restricted isometry constant* (RIC) associated with A.

Extension to images

We say that a linear operator $\mathcal{A} : \mathbb{C}^{n_1\times n_2} \to \mathbb{C}^m$ has the RIP of order s and level $\delta \in (0,1)$ if for all s-sparse $X \in \mathbb{C}^{n_1\times n_2}$, there holds

$$(1-\delta)\|X\|_2^2 \leq \|\mathcal{A}X\|_2^2 \leq (1+\delta)\|X\|_2^2.$$

Theorem 6.4.1

Assume the RIP of A and let δ_{3s} and δ_{4s} be the $3s$- and $4s$-RIC's of A, respectively, with $\delta_{3s} < 3(1-\delta_{4s}) - 1$. If

$$\alpha \leq \frac{\sqrt{1-\delta_{4s}}\sqrt{3s} - \sqrt{1+\delta_{3s}}\sqrt{s}}{(\sqrt{1-\delta_{4s}} + \sqrt{1+\delta_{3s}})\|x^{\text{opt}}\|_2},$$

then the minimizer x^{opt} of the springback problem satisfies

$$\|x^{\text{opt}} - \bar{x}\|_2 \leq \sqrt{\frac{2}{D_1}\tau + \frac{4}{\alpha}\|\bar{x} - \bar{x}_s\|_1},$$

where $D_1 = \dfrac{\alpha}{2}\dfrac{\sqrt{1-\delta_{4s}} + \sqrt{1+\delta_{3s}}}{\sqrt{3s} + \sqrt{s}}$.

Here $\bar{x}_s \in \mathbb{R}^n$ denotes the truncated vector corresponding to the s largest values of $\bar{x}$ (in absolute value).

- The CS theory for the springback model assumes the same RIP condition as that for the BP model, namely, $\delta_{3s} < 3(1-\delta_{4s}) - 1$.
- For the BP model and previous non-convex models, their reconstruction bounds take the form of

$$\|x^{\mathrm{opt}} - \bar{x}\|_2 \leq C_{1,s}\tau + C_{2,s}\frac{\|\bar{x} - \bar{x}_s\|_1}{\sqrt{s}},$$

- Comparison within the sparse regime, i.e., $\|\bar{x} - \bar{x}_s\|_1 = 0$:
  - ➥ The springback model has a **tighter** reconstruction bound than them in the sense of

$$\sqrt{\frac{2}{D_1}\tau} \leq C_s\tau$$

if the level of noise τ satisfies

$$\tau > \frac{2}{D_1 C_s^2}.$$

Let $\mathcal{H} : \mathbb{C}^{N\times N} \to \mathbb{C}^{N\times N}$ be the orthonormal bivariate Haar wavelet transform. Images are also **compressible** w.r.t. wavelet transforms:

Theorem 7.3.9

Let $N = 2^n$ with $n \in \mathbb{N}$. Assume $\mathcal{M} : \mathbb{C}^{N\times N} \to \mathbb{C}^m$ be such that the composite operator $\mathcal{M}\mathcal{H}^* : \mathbb{C}^{N\times N} \to \mathbb{C}^m$ has the RIP of order $Cs\log^3(N)$ and level $\delta < 0.6$. Let $\bar{X} \in \mathbb{C}^{N\times N}$ be a mean-zero image or an image containing some zero-valued pixels, and X^{opt} the solution to the enhanced TV model. If

$$\alpha \leq \frac{\sqrt{48s\log(N)}}{K_2\|\nabla X^{\text{opt}}\|_2},$$

then we have

$$\|\bar{X} - X^{\text{opt}}\|_2 \lesssim \sqrt{\frac{\sqrt{s}}{\alpha}\tau + \frac{1}{\alpha}\|\nabla\bar{X} - (\nabla\bar{X})_s\|_1}.$$

Needell and Ward 2013

The reconstruction error bound of the TV model (with RIP level $\delta < 1/3$):

$$\|\bar{X} - X^{\text{opt}}\|_2 \lesssim \frac{\|\nabla \bar{X} - (\nabla \bar{X})_s\|_1}{\sqrt{s}} + \tau.$$

To explore the scenarios where the bound of the enhanced TV model is **tighter** in the sense of

$$\sqrt{\frac{\sqrt{s}}{\alpha}\tau + \frac{1}{\alpha}\|\nabla \bar{X} - (\nabla \bar{X})_s\|_1} \lesssim \frac{\|\nabla \bar{X} - (\nabla \bar{X})_s\|_1}{\sqrt{s}} + \tau :$$

- Sparse regime $\|\nabla \bar{X} - (\nabla \bar{X})_s\|_1 = 0$: $\tau \gtrsim \frac{\sqrt{s}}{\alpha}$
- Noise-free regime $\tau = 0$: $\frac{s}{\|\nabla \bar{X} - (\nabla \bar{X})_s\|_1} \lesssim \alpha$

  LHS is an increasing function of s, and a limited number m of observations admits a small s

Pros and Cons of our new model

Pros:

- Benefited from non-convexity, our models do not introduce additional tricky implementation:

  In light of the difference-of-convex algorithm (DCA), we first linearize the subtracted convex term, and then solve a sequence of convex subproblems by ADMM.

- Our model enjoys tighter reconstruction error bounds in scenarios of less observations and/or larger noise level.

Cons:

- Achilles' Heel: the choice of α - our model may be unstable with an inappropriate alpha, but it always performs better than the convex model with an appropriate α.

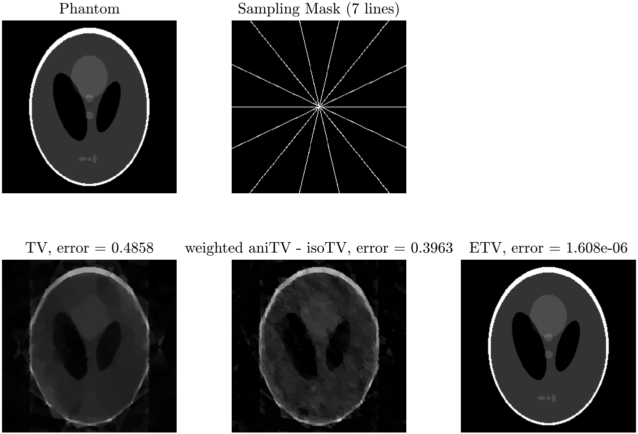

Figure: Reconstruction of 256×256 Shepp–Logan phantom.

Thanks for your attention.

Photo taken from Grass Island/Tap Mun, Hong Kong.